Comparison of the effects of platinum and CeO$_2$ on the properties of single grain, Sm–Ba–Cu–O bulk superconductors

You may also be interested in:

Comparison of the effects of platinum and CeO$_2$ on the properties of single grain, Sm–Ba–Cu–O bulk superconductors

Wen Zhao[1]**, Yunhua Shi**[1]**, Monika Radušovská**[2]**, Anthony R Dennis**[1]**, John H Durrell**[1]**, Pavel Diko**[2] **and David A Cardwell**[1]

[1] Bulk Superconductivity Group, Department of Engineering, University of Cambridge, CB2 1PZ, UK
[2] Laboratory of Materials Physics, Institute of Experimental Physics SAS, Košice, Slovakia

E-mail: wz268@cam.ac.uk

CrossMark

Abstract

SmBa$_2$Cu$_3$O$_{7-\delta}$ (Sm-123) is a light-rare-earth barium-cuprate (LRE-BCO) high-temperature superconductor (HTS) with significant potential for high field industrial applications. We report the fabrication of large, single grain bulk [Sm–Ba–Cu–O (SmBCO)] superconductors containing 1 wt% CeO$_2$ and 0.1 wt% Pt using a top-seeded melt growth process. The performance of the SmBCO bulk superconductors containing the different dopants was evaluated based on an analysis of their superconducting properties, including critical transition temperature, T_c and critical current density, J_c, and on sample microstructure. We find that both CeO$_2$ and Pt dopants refine the size of Sm$_2$BaCuO$_5$ (Sm-211) particles trapped in the Sm-123 superconducting phase matrix, which act as effective flux pinning centres, although the addition of CeO$_2$ results in broadly improved superconducting performance of the fully processed bulk single grain. However, 1 wt% CeO$_2$ is significantly cheaper than 0.1 wt% Pt, which has clear economic benefits for use in medium to large scale production processes for these technologically important materials. Finally, the use of CeO$_2$ results generally in the formation of finer Sm-211 particles and to the generation of fewer macro-cracks and Sm-211 free regions in the sample microstructure.

Keywords: high temperature superconductors, SmBCO, doping effects, comparison of Pt and CeO$_2$

(Some figures may appear in colour only in the online journal)

1. Introduction

Bulk, high-temperature superconductors (HTSs) of generic composition LRE-Ba–Cu–O (LRE-BCO), where LRE is a light rare earth element such as Nd, Sm, Gd, etc, fabricated in the form of large single grains, can potentially generate large magnetic fields compared to those produced by conventional permanent magnets, which are limited to below around 1.8 T. The field generating capacity of single grain bulk superconductors is determined primarily by the magnitude and homogeneity of the critical current density, J_c, of the material and the area over which it flows. The critical current depends essentially on the number, size and distribution of microscopic inhomogeneities throughout the macrostructure of the material [1]. Bulk SmBa$_2$Cu$_3$O$_{7-\delta}$ (Sm-123), which is a member of the LRE-BCO family of HTS, has significant potential for practical applications due to its high T_c and 'peak effect' characteristics in relatively high applied magnetic field [2, 3].

The growth of large Sm–Ba–Cu–O (SmBCO) single grains in air with good superconducting properties is difficult partly because SmBCO precursor powders have a high melting temperature, the choice of appropriate seeding material is limited. Additionally, the rapid growth rate of these

materials makes it difficult to optimise the conditions for successful grain growth. A further obstacle is that the superconducting properties of SmBCO bulk superconductors can be affected significantly by the substitution of Sm on the Ba site in the Sm-123 superconducting phase matrix [4]. In addition, the relatively poor mechanical properties of SmBCO single grains, in common with other LRE-BCO bulk super-conductors [5, 6], present a significant challenge to the development of a practical material for engineering applica-tions. Previous studies on Y–Ba–Cu–O (YBCO) bulk super-conducting samples indicate that Pt and CeO_2 refine the size and distribution of Y_2BaCuO_5 (Y-211) particles in the YBCO single grains, which correlates with an increase in trapped magnetic flux density and J_c [7]. However, to date, compar-able research has not yet been performed on SmBCO. Izumi *et al* demonstrated that the addition of Pt, introduced as a contaminant from the crucible during the first partial melting step in the so-called melt powder melt growth method, is effective in refining Y-211 particles in the fully processed single grain [8]. Kim *et al* reported subsequently that needle-like and highly anisotropic Y-211 particles form in single grain YBCO samples containing Pt, whereas samples pro-cessed with CeO_2 contain finer Y-211 particles with reduced anisotropy [7, 9]. More recently, Diko *et al* have investigated and compared further the effect of these additions on the properties of single grains. The effect of Pt and CeO_2 on the aggregation of Y-211 particles in single grain YBCO samples and the microstructures of samples containing the two dif-ferent dopants, in particular, have been studied and compared fully [10, 11]. Furthermore, Muralidhar *et al* extended the study into the (Nd, Eu, Gd)–Ba–Cu–O (NEG-BCO) system, which is more analogous to the SmBCO system. To sum-marise, they succeeded in enhancing J_c of the NEG-BCO system through the refinement of 211 particles by combined addition of Pt and CeO_2 [12, 13]. Finally, since CeO_2 is much cheaper than Pt, it forms a highly desirable alternative in the large-scale production of bulk LRE-BCO superconductors for commercially viable applications.

This research compares the comparative merits of the addition of Pt and CeO_2 in improving the superconducting and mechanical properties of SmBCO bulk single grains fabricated using the top-seeded melt growth (TSMG) tech-nique. We have investigated the microstructural modifications associated with Pt or CeO_2 addition to the precursor powder and discuss the effect of these additions on the size and the morphology of Sm_2BaCuO_5 (Sm-211) particles in the fully processed SmBCO single grain.

2. Experimental

Commercially available precursor powders were used to fabricate SmBCO bulk single grains. Both SmBCO + CeO_2 and SmBCO + Pt precursors contained 75 wt% Sm-123 (Toshima, average particle size: 2–3 μm), 25 wt% Sm-211 (Toshima, average particle size: 1–2 μm) and 2 wt% BaO_2 (Sigma-Aldrich, purity 95%; to suppress Sm/Ba substitution [14]). 1 wt% CeO_2 (Sigma-Aldrich, purity 99.9%) and
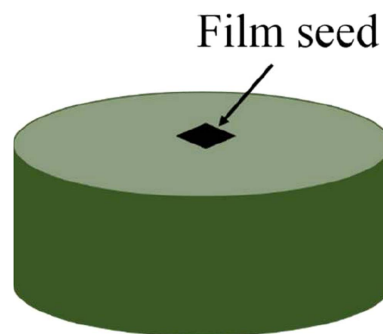

Figure 1. Schematic illustration of the bulk pre-form with the thin film seed.
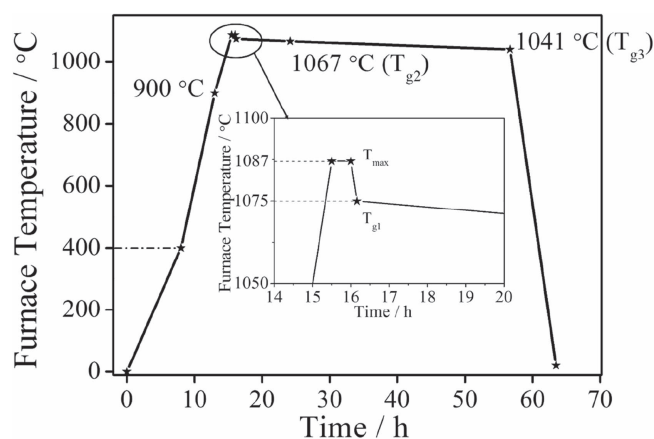

Figure 2. Heating profile used to produce single grain samples of the various SmBCO compositions.

0.1 wt% Pt (Alfa Aesar, purity 99.98%, 350 mesh) were added subsequently to each precursor powder, which is the optimised amount in our group [15]. The powders were then pressed uniaxially under a load of 1.5 tons in a cylindrical die of diameter 20 mm. Pellet pre-forms of thickness 9 mm were obtained for each composition (each pellet shrinks to about 80% of its original size after TSMG, corresponding approximately to as-processed dimensions of 16 mm diameter and 7 mm thickness). Pure SmBCO containing only Sm-123 and Sm-211 was also prepared for purposes of comparison using the same TSMG procedure for precursor samples of comparable overall volume and weight.

A thin film seed [16] consisting of NdBCO of thickness 700 nm deposited on a single crystal MgO-substrate provided by Ceraco was placed at the centre of the top surface of the as-prepared pre-forms to control single grain nucleation and growth in the required orientation, as illustrated schematically in figure 1.

The TSMG method based on the heating profile shown in figure 2 was used to fabricate the bulk, single grains of the various compositions in air. Initially, the temperature was raised slowly to 400 °C at a rate of 50 °C h^{-1}, followed by a more rapid increase to 900 °C to stabilise the film seed. The temperature was then increased further to 1087 °C (T_{max}) and held at this level for 0.5 h to allow the precursor pellet to decompose. The sample was then cooled in three stages.
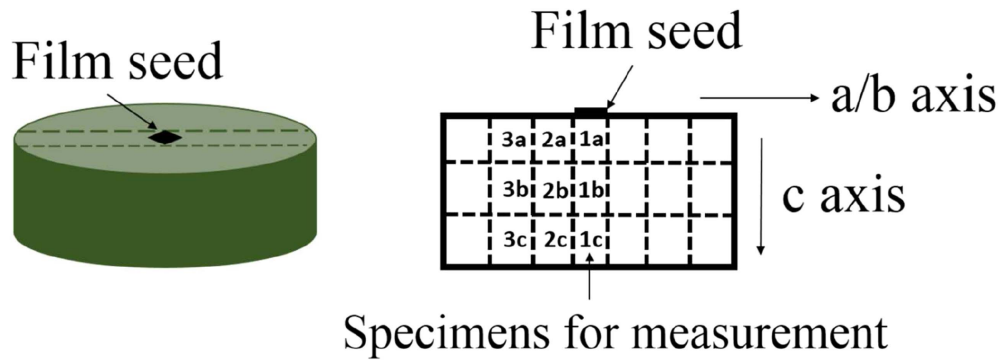
Figure 3. Schematic illustration of the position of the bulk specimens within the as-processed single grain.

Firstly, the furnace temperature was decreased to 1075 °C (T_{g1}) at a rate of 75 °C h^{-1} and then to 1067 °C (T_{g2}) at a rate of 1 °C h^{-1}. The solidification procedure was completed by reducing the temperature to 1041 °C (T_{g3}) at the rate of 0.8 °C h^{-1}. Finally, the samples were furnace cooled to room temperature at a rate of 150 °C h^{-1}.

The as-grown samples were oxygenated at 360 °C for fourteen days to drive the non-superconducting, tetragonal Sm-123 phase to the desired orthorhombic, superconducting phase.

Differential thermal analysis (DTA) was performed using a Setaram LabSYS Evo instrument on the SmBCO + CeO$_2$ and SmBCO + Pt precursor powders. A small, generic seed [17] was placed at the centre of the top surface of the small pellet mimicking the bulk pre-form to simulate the TSMG process at elevated temperature in order to determine the various growth-related temperatures for use in the full melt process.

Each sample was cut in half using a diamond saw, as illustrated schematically in figure 3. One half of each bulk SmBCO cross-section was polished for microstructural observation using a polarised light microscope (Nikon, model ECLIPSE ME600), and the other half was prepared for measurement using a SQUID magnetometer (Superconducting Quantum Interference Device Magnetometer, Quantum Design, model MPMS-XL). The spatial variation in T_c was investigated on sub-specimens of size approximately 1.5 mm × 2.0 mm × 1.2 mm cutting systematically from equivalent locations within each parent single grain, as shown schematically in figure 3, using a field of 0.002 T applied parallel to the *c*-axis of each sub-specimen. J_c was calculated subsequently using the extended Bean model [18] from the measured M-H hysteresis loops at 77 K.

Scanning electron microscopy was used to investigate the microstructure of each sub-specimen, with chemical analysis being performed simultaneously by energy dispersive x-ray spectrometry (EDX).

3. Results and discussion

DTA was performed in order to estimate the peritectic reaction temperatures of the SmBCO precursor powders containing CeO$_2$ and Pt to simulate the TSMG process at elevated
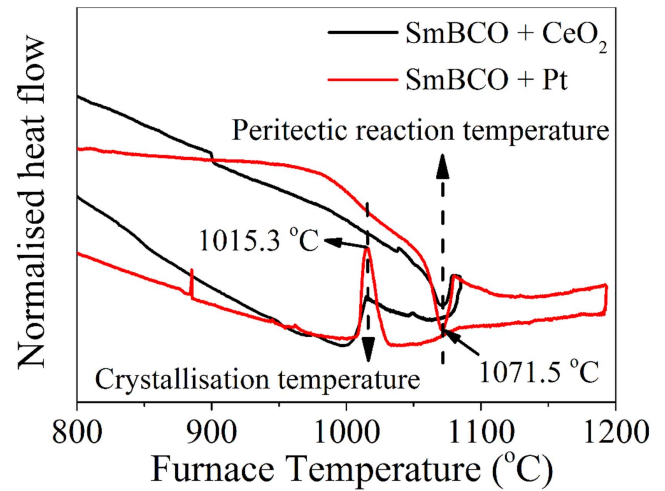

Figure 4. Diffrential thermal analysis traces of SmBCO + CeO$_2$ and SmBCO + Pt precursor powders.

temperature. The peak values identified subsequently in figure 4 were then used as the corresponding peritectic reaction and crystallisation temperatures. It is clear from this figure that both compositions exhibit similar values of these key process parameters in that each precursor powder decomposes at around 1071.5 °C and crystallises at around 1015.3 °C theoretically at equilibrium state, which allows the same heating profile to be used to grow these samples. This, in turn, makes subsequent comparison of the properties of the single grains much more meaningful. As a result, combining further knowledge of the growth kinetics and fabrication of the SmBCO system, T_{max} in the heating profile was set to 1087 °C rather than the peritectic reaction temperature, 1071 °C, to ensure decomposition of the precursor powders. Additionally, a growth temperature T_{g3} is established to 1041 °C, which is higher than the crystallisation temperature to guarantee a wide growth window, which is beneficial to successful sample growth.

Photographs of successfully grown single grains of diameter 16 mm for SmBCO containing CeO$_2$ and Pt are shown in figure 5. Both samples were synthesised in the same batch, prepared using the same furnace and heating profile and
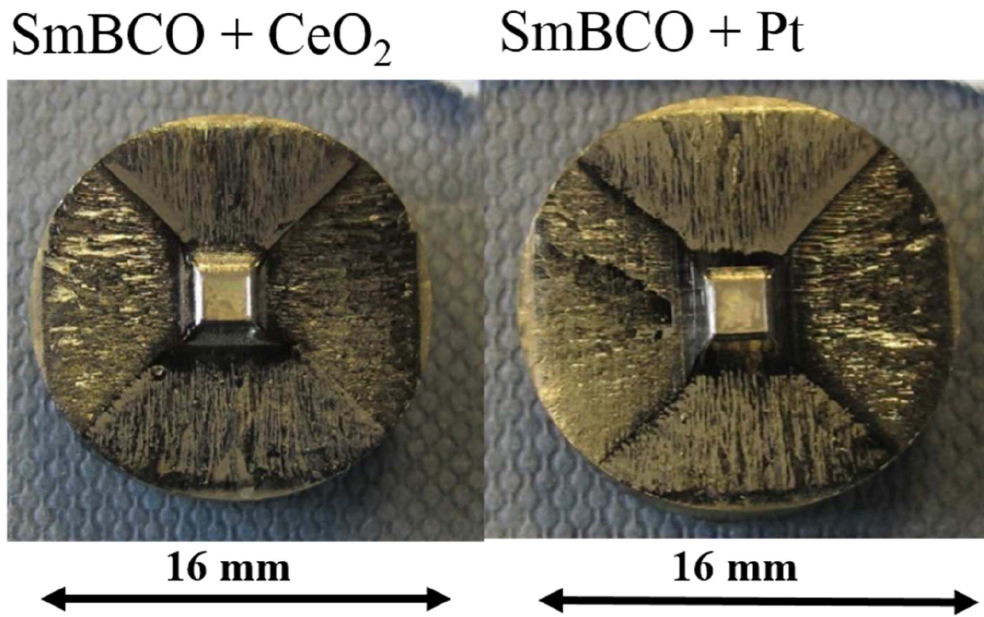
Figure 5. Photographs of the top surfaces of SmBCO + CeO$_2$ and SmBCO + Pt single grains.

Figure 6. Comparison of T_c for the sub-specimens along the a/b-axis and c-axis of the SmBCO + CeO$_2$ and SmBCO + Pt single grains.

Figure 7. Comparison of T_c for specimens at the same position in the parent single grain for $SmBCO + CeO_2$ and $SmBCO + Pt$ compositions.
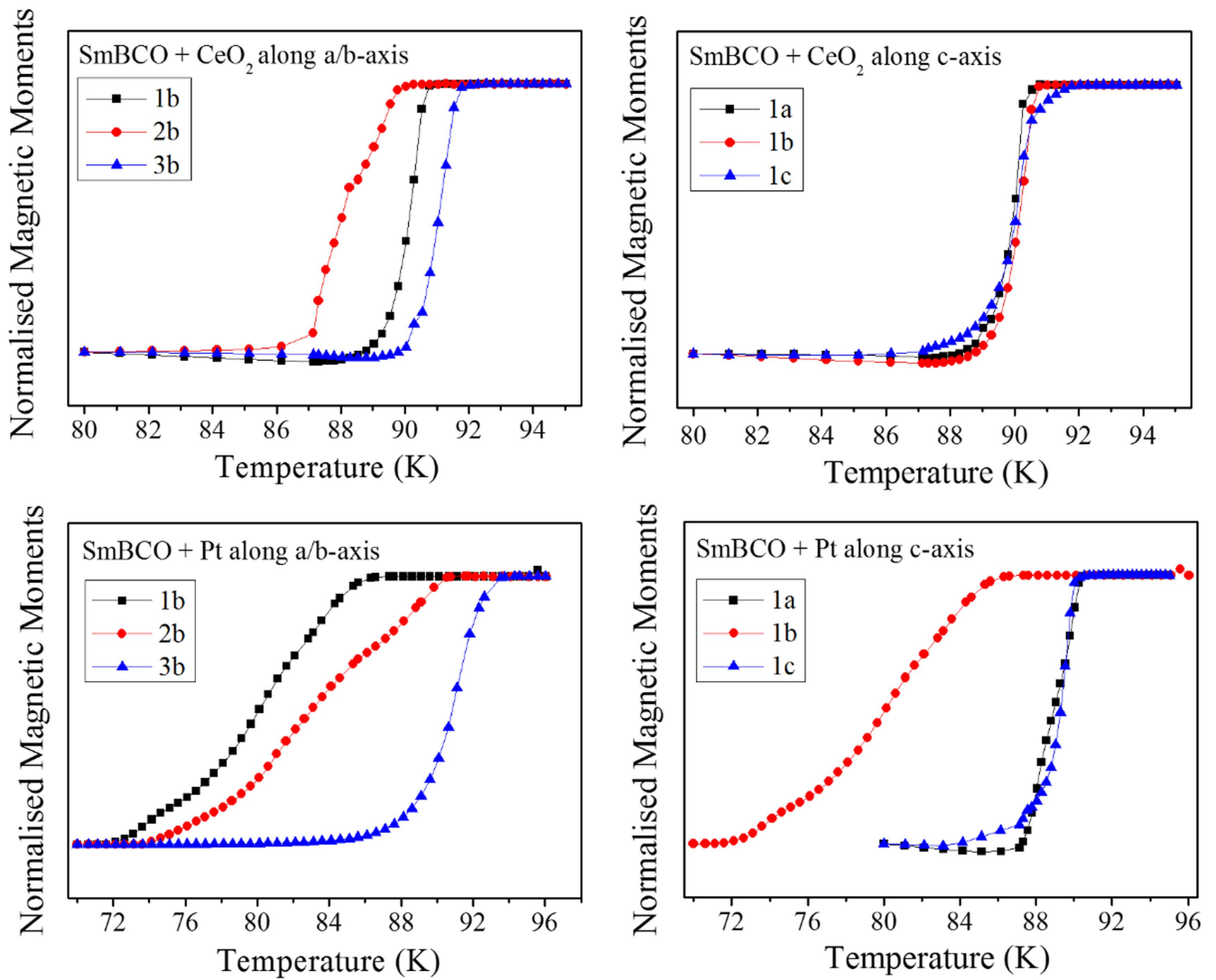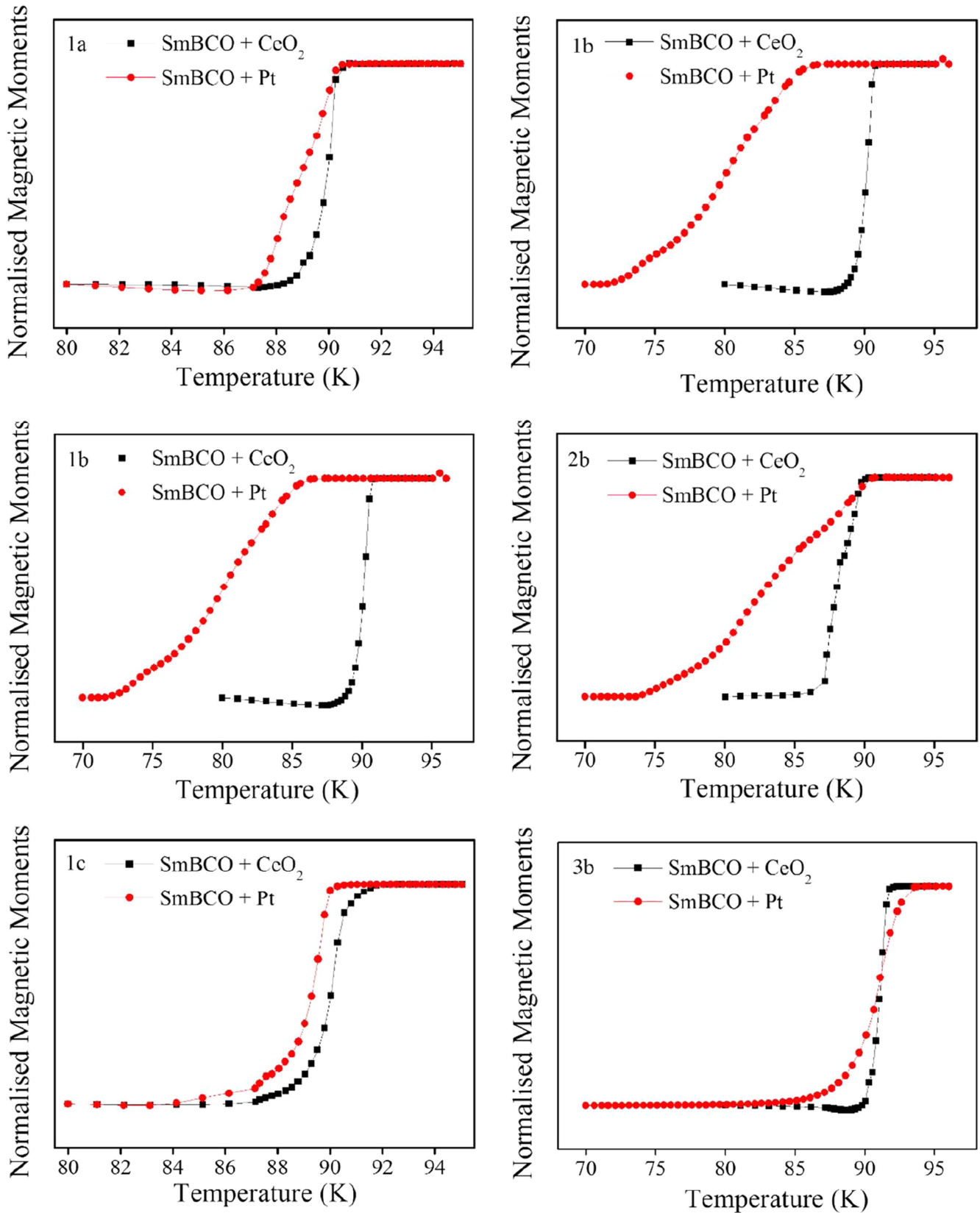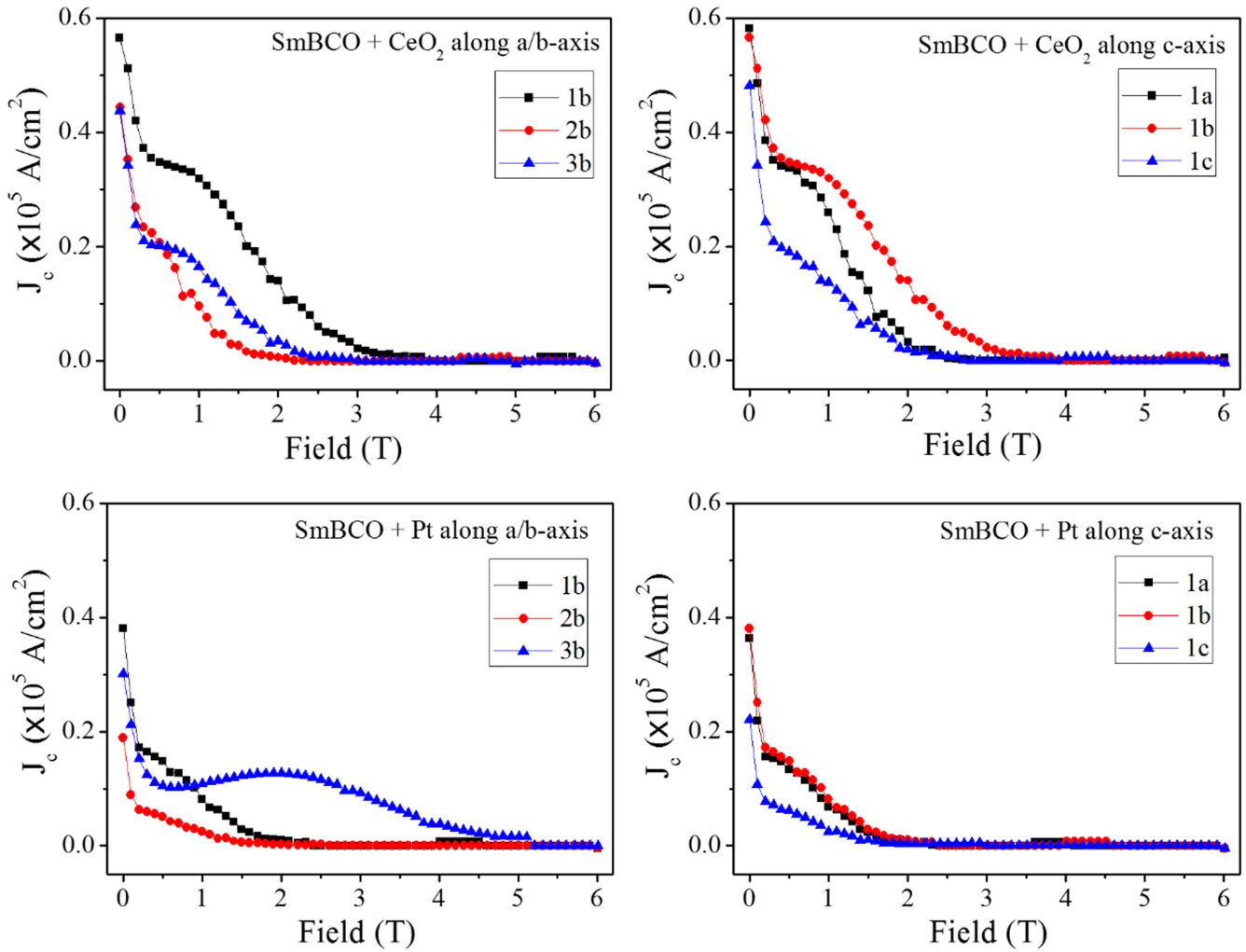
Figure 8. Comparison of J_c for the sub-specimens along the a/b-axis and c-axis of the SmBCO + CeO$_2$ and SmBCO + Pt single grains.

oxygenated under the same conditions. It can be seen that four, clear growth facet lines extend from the seed to the edges of each sample, indicating that each is grown fully by TSMG in air in the form of a large, single grain.

The variation of T_c along both crystallographic axes and at different locations with the bulk single grain are compared for the different sample compositions in figure 6. By considering T_c and the observed transition width, ΔT_c, it can be concluded that the variation in superconducting properties is greater for both sets of sub-specimens along the a/b-axis than along the c-axis, independently of whether the sample is composed of SmBCO + CeO$_2$ or SmBCO + Pt.

The T_c of SmBCO is affected significantly by substitution of Ba by Sm in the Sm-123 phase matrix [4]. This effect can vary with sample position if we assume that the concentration of Sm in the melt increases with the distance from the seed, which may lead to more severe substitution effects of Ba by Sm. The melt composition in SmBCO + CeO$_2$ and SmBCO + Pt will be different, because the reaction of CeO$_2$ with the Sm-123 phase generates an excess of CuO in the melt, which will therefore increase with distance from the seed and potentially influence the extent of Sm/Ba substitution [19].

In figure 7, comparison of the T_c of the sub-specimens at equivalent positions in the two single grain samples at the five positions measured along the a/b-axis and c-axis in this study indicates clearly that the sample fabricated from SmBCO + Pt is not as good as that containing SmBCO + CeO$_2$. The data indicate a lower T_c and a broader ΔT_c in the former, with only one exception at position 3b, where a higher T_c was observed in the SmBCO + Pt single grain. However, it should be noted that ΔT_c at this position in the SmBCO + Pt sample is also much broader than that in SmBCO + CeO$_2$. As a result, such a high local T_c does not contradict the general conclusion that the effect of the addition of Pt to SmBCO is not as beneficial to its superconducting properties as the addition of CeO$_2$.

J_c at 77 K calculated using the extended Bean model [18] for the specimens along the a/b-axis and c-axis of each sample are shown in figure 8. Although there is significant variation with position, J_c is consistently higher in the single grain sample containing CeO$_2$. In addition, no regular trends are apparent in these data, and the sub-specimens exhibit different J_c values in both samples along the a/b- and c- axes as shown in figure 3, with different associated peak effects and irreversibility fields.
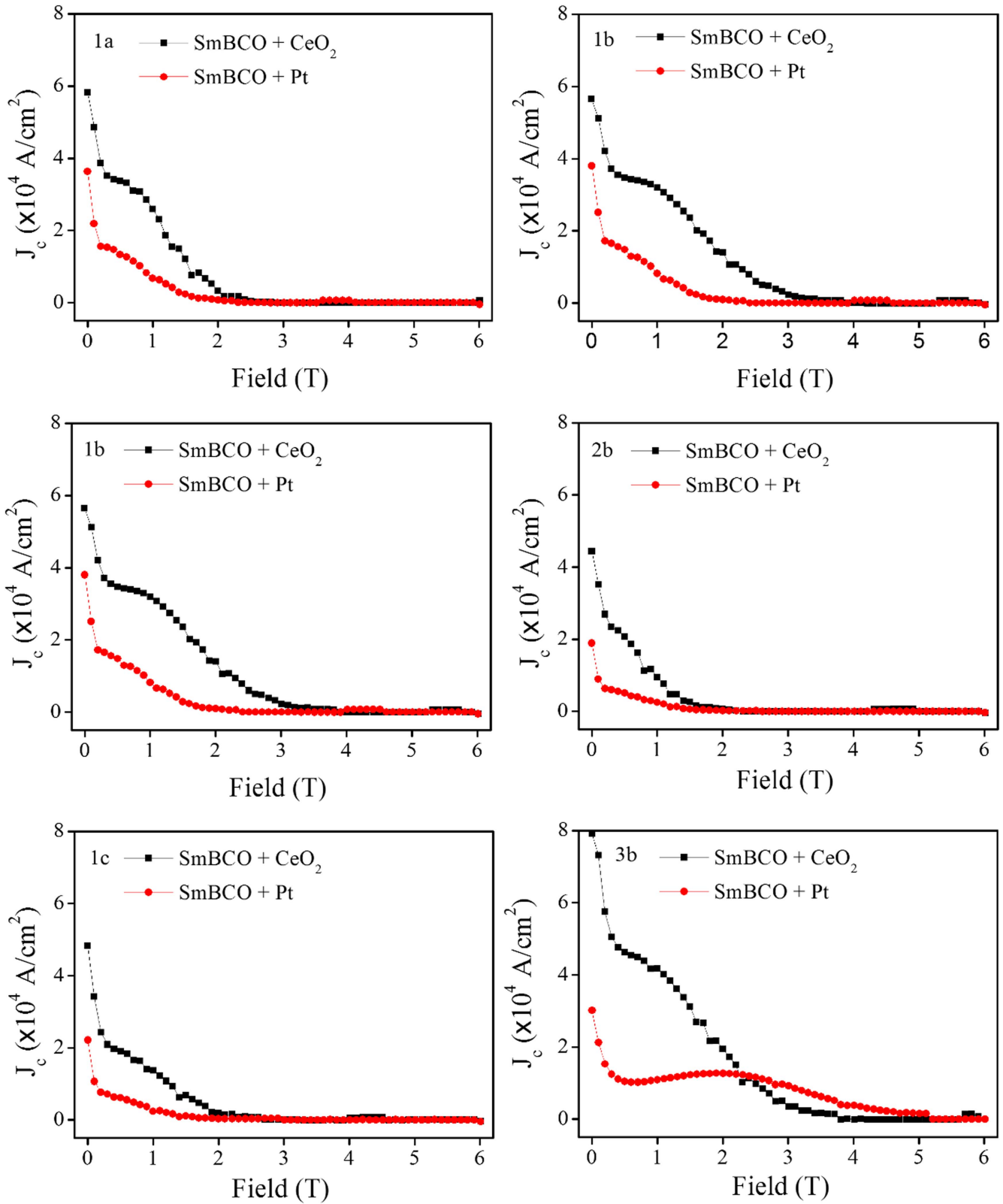
Figure 9. Comparison of J_c for specimens at the same position in the parent single grain for SmBCO + CeO$_2$ and SmBCO + Pt compositions.

Figure 9 shows a comparison of J_c for the specimens at the same locations in the parent single grain for the two sample compositions. Although the values of J_c vary from position to position, generally speaking the sample containing SmBCO + CeO$_2$ exhibits a more pronounced peak effect and higher irreversibility field than the sample containing SmBCO + Pt across the entire cross-section of the single grain.

Further microscopic studies were performed on the single grain samples in an attempt to explain the differences in J_c

(1) SmBCO + CeO$_2$

(2) SmBCO + Pt

(3) Pure SmBCO

(4) SmBCO + CeO$_2$

(5) SmBCO + Pt

20 μm
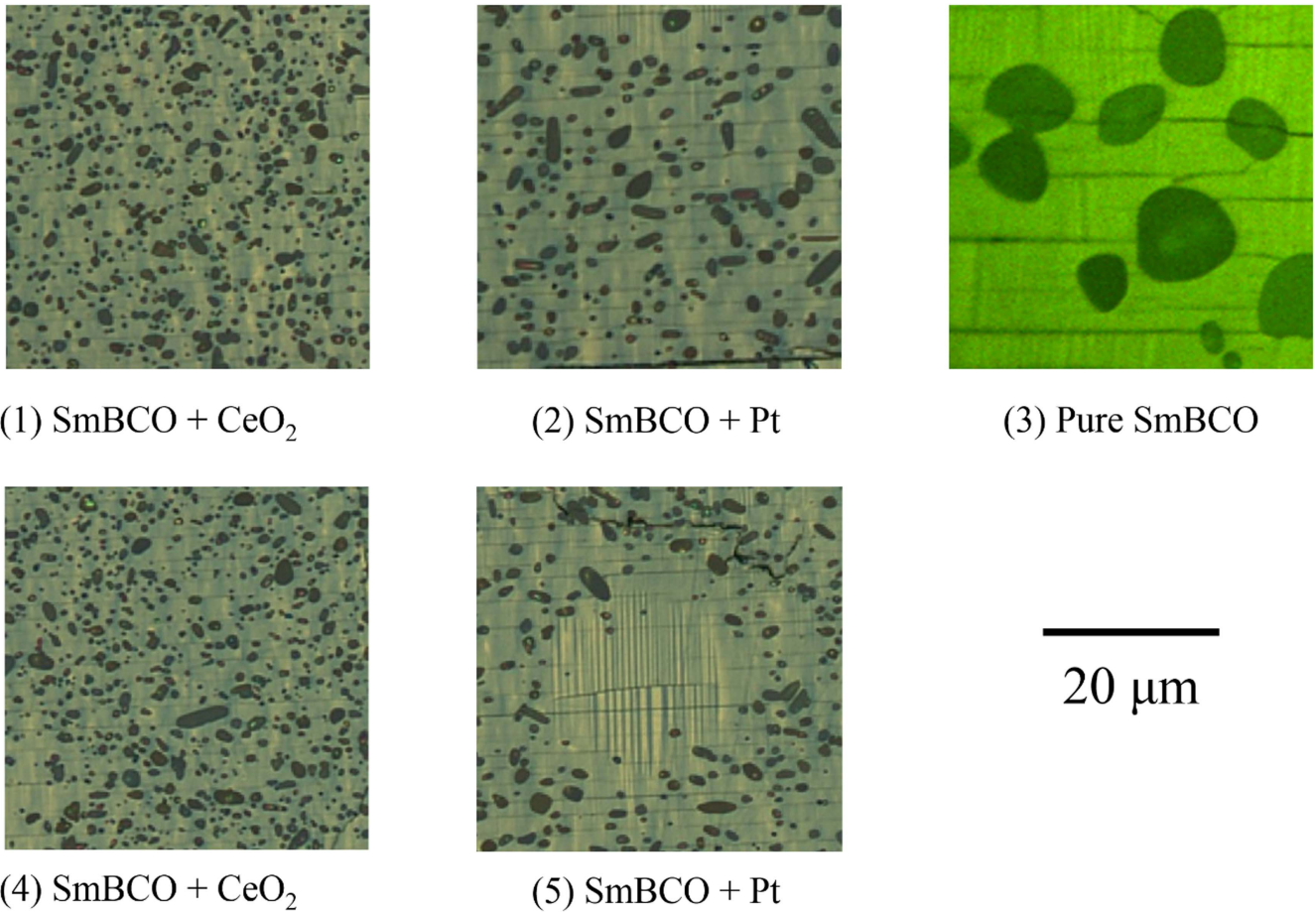
Figure 10. Micrographs at a magnification of 500× for the SmBCO + CeO$_2$ ((1) and (4)) and SmBCO + Pt samples ((2) and (5)) observed at equivalent positions in the parent single grain (1b position in figure 3). Micrograph (3) is for the undoped single grain SmBCO sample (pure SmBCO).

Figure 11. EDX analysis of the Ce-containing second phase located on macro-cracks formed orthogonally to the *c*-axis in the single grain sample of composition SmBCO + CeO$_2$.

Figure 12. EDX analysis of the Ce-containing second phase formed in pores in the single grain sample of composition SmBCO + CeO$_2$.

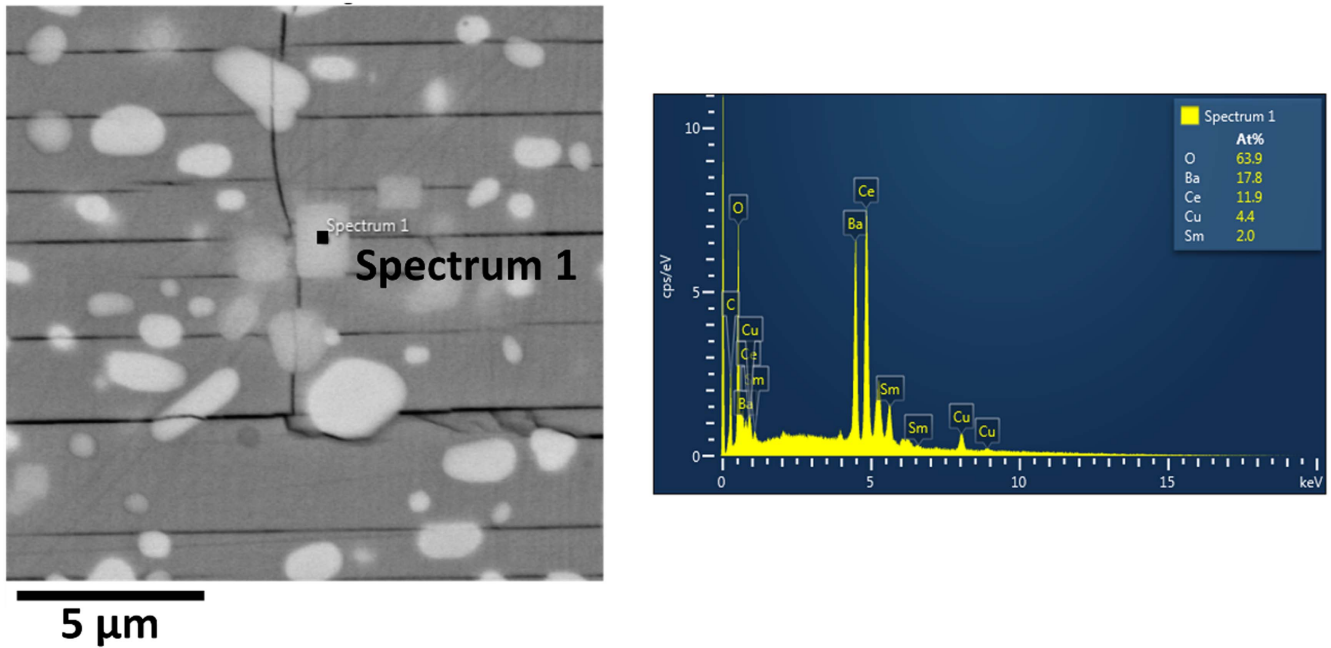**Table 1.** Summary of the EDX analysis for the Ce-containing second phase located on macro-cracks formed orthogonally to the *c*-axis in the single grain sample of composition SmBCO + CeO$_2$.
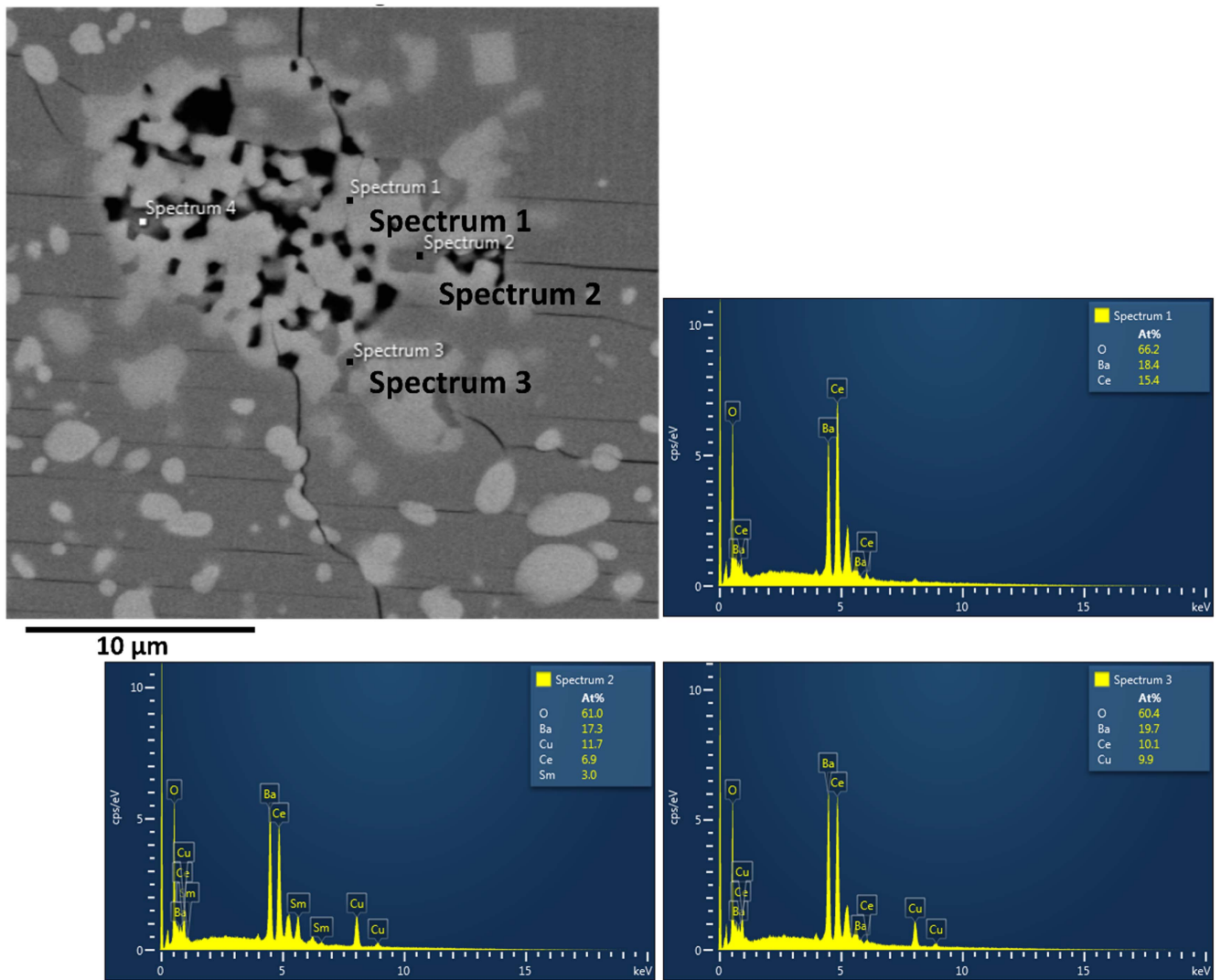
Spectrum no.	Element amount detected/At.%				
	Ba	Ce	O	Sm	Cu
Spectrum 1	17.8	11.9	63.9	2.0	4.4

Table 2. Summary of the EDX analysis for the Ce-containing second phase formed in pores in the single grain sample of composition SmBCO + CeO$_2$.

Spectrum no.	Element amount detected/At.%				
	Ba	Ce	O	Sm	Cu
Spectrum 1	18.4	15.4	66.2	—	—
Spectrum 2	17.3	6.9	61.0	3.0	11.7
Spectrum 3	19.7	10.1	60.4	—	9.9

between these samples given that this parameter is related closely to the ability of the single grain to pin magnetic flux lines, and therefore to generate increased trapped field. This, in turn, is determined variously by inhomogeneities in the sample microstructure, such as micro-cracks, LRE-211 particle inclusions and twin planes, etc [1].

Kim *et al* reported that both Pt and CeO$_2$ are capable of refining the size of the LRE-211 particles in the LRE-BCO single grain microstructure [7], which is further confirmed in this study. Micrographs (1), (2) and (3) in figure 10 exhibit different Sm-211 particle sizes in the three compositions investigated [(SmBCO + CeO$_2$, SmBCO + Pt and undoped SmBCO (pure SmBCO)]. The largest Sm-211 particle size observed in single grain samples fabricated without the addition of either CeO$_2$ or Pt can be as high as 10 μm, which is more than 5 times the size of those observed in the compositions containing CeO$_2$ or Pt.

Micrographs (1), (2), (4) and (5) in figure 10 reveal that the presence of CeO$_2$ refines the Sm-211 particles further, so

that a smaller average Sm-211 particle size is observed in these materials. The Sm-211 particles are also much better distributed across the entire cross-section of the single grain in SmBCO + CeO$_2$ compared to SmBCO + Pt. The inferior superconducting properties in SmBCO + Pt may be attributed, in part, to the presence of a relatively large number of Sm-211 free regions, as shown in figure 10(5), which is not observed in the SmBCO + CeO$_2$ samples.

The results of the EDX analysis are summarised in figures 11 and 12, and tables 1 and 2. These indicate that CeO$_2$ exists mainly in the single grain bulk in the form of BaCeO$_3$ (the trace amount of Sm and Cu is due to the background signal from the bulk matrix), which is consistence with the findings in previous study in YBCO system [10]. The rectangular BaCeO$_3$ particles are homogenously distributed in the bulk and their size is comparable with the size of Sm-211 particles, so they can positively contribute to pinning. The images also give information on the distribution of BaCeO$_3$ in the single grain. The particles tend to form agglomerates generally in pores or in the vicinity of macrocracks, which limits the propagation of the latter under an applied stress (their stoichiometry can be estimated by EDX more closely to BaCeO$_3$). This, in turn, leads to the formation of fewer micro-cracks, which prohibit the flow of the supercurrent through the bulk single grain. Such a distribution of second phase inclusions, on the other hand, cannot be found in the SmBCO samples containing Pt. This could account further for the superior superconducting properties observed for the SmBCO sample containing CeO$_2$.

The cost of the addition of Pt and CeO$_2$ to the bulk material should be compared to establish the economic viability of the single grain fabrication process. The price of the commercially available CeO$_2$ (Sigma-Aldrich, purity 99.9%, 100 g) and Pt (Alfa Aesar, purity 99.98%, 350 mesh, 5 g) chemicals used in this study was £ 37.20 and £ 767.00, respectively. As a result, 1 wt% of CeO$_2$ (£ 0.372 g^{-1}) costs less than one 40th of 0.1 wt% of Pt (£ 153.4 g^{-1}). Hence, the SmBCO + CeO$_2$ single grain exhibits superior superconducting properties at significantly lower cost, which demonstrates clearly that CeO$_2$ is not only a better candidate as a secondary phase refiner than Pt, but is also a more economic option for production of single grain SmBCO samples for commercially viable applications.

4. Conclusions

We have successfully fabricated bulk, single grain SmBCO samples in air with Pt and CeO$_2$ additions. Comparison of the measured superconducting properties of both single grain compositions has shown clearly that CeO$_2$ is more effective at refining the secondary Sm-211 phase inclusions in the bulk microstructure than Pt. Microstructural analysis of the two single grains has indicated further that the SmBCO + CeO$_2$ sample contains fewer macro cracks, finer Sm-211 particles and a more homogeneous Sm-211 distribution within the parent single grain, which, collectively, contribute to better bulk superconducting performance for this composition.

Finally, the addition of CeO$_2$ is significantly more cost effective than the addition of Pt, which is important for the development of a commercially viable single grain fabrication process. We conclude for the first time, therefore, that CeO$_2$ offers significant performance and commercial benefits over Pt to improving the superconducting, mechanical and cost efficiency properties of large, single grain SmBCO for practical applications.

References

[1] Cardwell D A 1998 Processing and properties of large grain (RE)BCO *Mater. Sci. Eng.* B **53** 1–10

[2] Murakami M, Yoo S, Higuchi T, Sakai N, Weltz J, Koshizuka N and Tanaka S 1994 Flux pinning in melt-grown NdBa$_2$Cu$_3$O$_y$ and SmBa$_2$Cu$_3$O$_y$ superconductors *Japan. J. Appl. Phys.* **715** L715–7

[3] Hari Babu N, Iida K, Shi Y and Cardwell D A 2008 Processing of bulk Sm–Ba–Cu–O nano-composite superconductors *Physica* C **468** 1340–4

[4] Sun L, Li W, Liu S, Mertelj T and Yao X 2009 Growth of a high performance SmBCO bulk superconductor with the addition of a Sm$_2$Ba$_4$Cu$_2$O$_9$ phase *Supercond. Sci. Technol.* **22** 125008

[5] Konstantopoulou K, Shi Y H, Dennis A R, Durrell J H, Pastor J Y and Cardwell D A 2014 Mechanical characterization of GdBCO/Ag and YBCO single grains fabricated by top-seeded melt growth at 77 and 300 K *Supercond. Sci. Technol.* **27** 115004

[6] Sakai N, Mase A, Ikuta H, Seo S, Mizutani U and Murakami M 2000 Mechanical properties of Sm–Ba–Cu–O/Ag bulk superconductors *Supercond. Sci. Technol.* **13** 770–3

[7] Kim C, Kim K and Hong G 1994 Y$_2$BaCuO$_5$ morphology in melt-textured Y–Ba–Cu–O oxides with PtO$_2$·H$_2$O/CeO$_2$ additions *Physica* C **232** 163–73

[8] Izumi T, Nakamura Y, Sung T-H and Shiohara Y 1992 Reaction mechanism of Y-system superconductors in the MPMG method *J. Mater. Res.* **7** 801–7

[9] Kim C, Kim K, Kuk I and Hong G 1997 Role of PtO$_2$ on the refinement of Y$_2$BaCuO$_5$ second phase particles in melt-textured Y–Ba–Cu–O oxides *Physica* C **281** 244–52

[10] Diko P, Šefčíková M, Kaňuchová M and Zmorayová K 2008 Microstructure of YBCO bulk superconductors with CeO$_2$ addition *Mater. Sci. Eng.* B **151** 7–10

[11] Diko P, Wende C, Litzkendorf D, Klupsch T and Gawalek W 1998 The influence of starting YBa$_2$Cu$_3$O$_{7-x}$ particle size and Pt/Ce addition on the microstructure of YBa$_2$Cu$_3$O$_{7-x}$–Y$_2$BaCuO$_5$ melt processed bulks *Supercond. Sci. Technol.* **11** 49–53

[12] Muralidhar M, Koblischka M R and Murakami M 2000 (Nd, Eu, Gd)–Ba–Cu–O superconductors with combined addition of CeO$_2$ and Pt *Supercond. Sci. Technol.* **13** 693–7

[13] Muralidhar M, Jirsa M, Nariki S and Murakami M 2001 Influence of combined Pt and CeO$_2$ additions on microstructure and magnetic properties in (Nd, Eu, Gd)–Ba–Cu–O *Supercond. Sci. Technol.* **14** 832–8

[14] Babu N H, Shi Y, Iida K and Cardwell D A 2005 A practical route for the fabrication of large single-crystal (RE)–Ba–Cu–O superconductors *Nat. Mater.* **4** 476–80

[15] Mancini C E 2012 The development of high quality, cost-effective bulk superconductors for production processes *Masters Thesis* University of Cambridge

[16] Chen Y, Cui X and Yao X 2015 Peritectic melting of thin films, superheating and applications in growth of REBCO superconductors *J. Prog. Mater. Sci.* **68** 97–159

[17] Shi Y, Babu N H and Cardwell D A 2005 Development of a generic seed crystal for the fabrication of large grain (RE)–Ba–Cu–O bulk superconductors *Supercond. Sci. Technol.* **18** L13–6

[18] Chen D X and Goldfarb R B 1989 Kim model for magnetization of type-II superconductors *J. Appl. Phys.* **66** 2489–500

[19] Volochova D, Diko P, Antal V, Radusovska M and Piovarci S 2012 Influence of Y$_2$O$_3$ and CeO$_2$ additions on growth of YBCO bulk superconductors *J. Cryst. Growth* **356** 75–80